Tidal Exchange through a Strait: A Numerical Experiment Using a Simple Model Basin

TOSHIYUKI AWAJI, NORIHISA IMASATO AND HIDEAKI KUNISHI

Geophysical Institute, Kyoto University, Kyoto, Japan

(Manuscript received 14 November 1979, in final form 25 April 1980)

ABSTRACT

In order to investigate the mechanism of tidal exchange through a strait, we numerically track the Lagrangian movement of water particles over a full cycle of the M_2 tide. As a result, it is found that the spatially rapid changes of the amplitude and the phase lag of the M_2 current in the vicinity of the strait cause the exchange of an extremely large amount of water through the strait. The tidally-induced residual circulation in the vicinity of the strait also plays an important role in the water exchange. The calculated exchange ratio over one tidal cycle is ~87%, i.e., the greater part of the outer water entering into the inner basin through the strait stays in the inner basin while an equal amount of basin water is drawn out after a cycle of the M_2 tide. This fact also suggests that the major part of the water exchange through a strait is generated, not by turbulent diffusion, but by the dynamic process of the tidal current.

1. Introduction

The problem of tidally-induced net exchange of water between basins connected by a narrow strait has been of interest for many years. In such studies it has been necessary to invoke assumptions concerning the horizontal spread of intruding water and of the degree of mixing to arrive at estimates of net exchange (Parker *et al.*, 1972; Kawamura *et al.*, 1975; Nakata *et al.*, 1976). In order to clarify the problem and to reveal the mechanism of tidal exchange, we undertake a numerical experiment in which we track a large number of labeled particles released in the current driven by the M_2 tide over a complete cycle.

In the study of water waves, it has been long known that Stokes waves are attended by the so-called Stokes drift induced by velocity shear. This well-known phenomenon suggests that if a marked particle is released in a tidal current with strong horizontal shear, the particle should not return to its starting point after a cycle of the tide. Moreover, we can predict the same result if there exists spatially rapid changes of phase lag of the tidal current, because it plays a similar role to the horizontal velocity shear of the tidal current. These spatially rapid changes of the amplitude and the phase lag of the tidal current are induced by friction and by the rapid variation of the coastal geometry. Therefore, in an actual sea, water particles in the vicinity of a strait will ordinarily have large drifts.

We assume a situation where the inner water (water being initially in an inner basin such as the left basin in Fig. 1) and the outer water (water being initially in an outer basin such as the right basin in Fig. 1) are divided by a boundary (chain line in Fig. 1) across a strait. Then some particles of the inner and outer waters in the vicinity of the strait will drift over a large area and their trajectories will not be closed after a cycle of the M_2 tide; as a result fairly large amounts of water are exchanged between the inner and outer basins through the strait.

In order to obtain the drifts of water particles, in the present paper, the trajectories of a large number of labeled particles are calculated by integrating the Lagrangian (particle's) velocities approximately obtained from the Eulerian velocity field of the tidal current. This Euler-Lagrange problem was studied by Longuet-Higgins in 1969, when he investigated the Lagrangian drift of a marked particle in a periodic current. The exchanged volume of water between these two basins is evaluated from the calculated distribution of the particles.

One of the most important problems in environmental preservation in coastal seas is to reveal the details of the Lagrangian movement of water particles. As a first step in approaching the problem, in the present paper, we study the mechanism of tidal exchange through a strait by using the Euler-Lagrange method.

2. Formulation of the problem

We consider the horizontal two-dimensional movement of marked particles in a simple model basin, which is a convenient way to study the physical processes of the phenomena. The model basin has a simple geometry, shown in Fig. 1, and consists of two basins, inner and outer, connected to each other by a strait, 5 km in length and 4 km in

0022-3670/80/101499-10$06.50

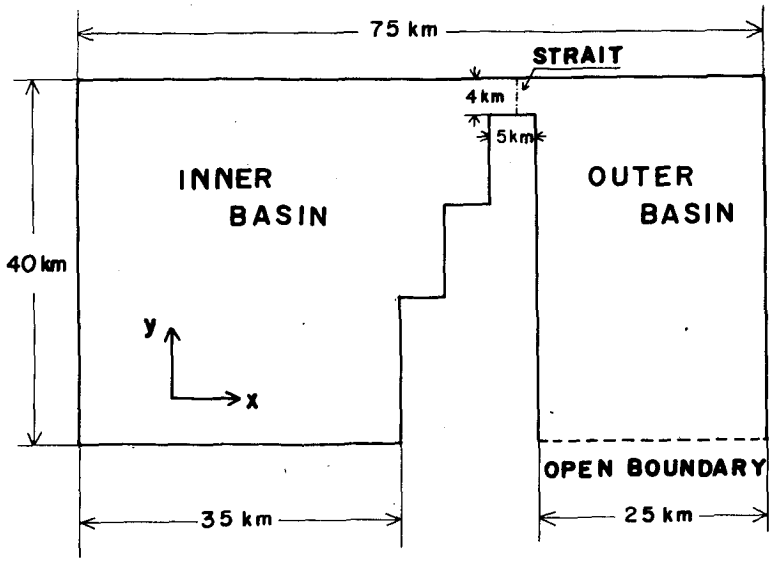

FIG. 1. Schematic view of the model basin.

width. The outer basin also has an open boundary (broken line in Fig. 1), where the amplitude and the phase lag of the M_2 tide are specified. The bottom of the model basin is flat and is 40 m below the mean sea level.

The Eulerian velocity field driven by the M_2 tide is obtained as follows. The vertically averaged, horizontal, two-dimensional equations of motion and continuity are

$$\frac{\partial \mathbf{u}}{\partial t} + \mathbf{u}\cdot\nabla_H\mathbf{u} + f\mathbf{k}\times\mathbf{u} = -g\nabla_H\zeta + \nu_H\nabla_H{}^2\mathbf{u} + \frac{\tau}{H+\zeta}, \quad (1)$$

$$\frac{\partial \zeta}{\partial t} = -\nabla_H\cdot\{(H+\zeta)\mathbf{u}\}, \quad (2)$$

where we have assumed a hydrostatic balance in a homogeneous fluid. The operator ∇_H is $\mathbf{i}\partial/\partial x + \mathbf{j}\partial/\partial y$ and $\nabla_H{}^2$ is $\partial^2/\partial x^2 + \partial^2/\partial y^2$. $\mathbf{u}$ is the vertically averaged horizontal velocity vector with components u and v in the Eulerian system of coordinates x and y as shown in Fig. 1, ζ the height of water surface above the mean sea level, H the depth of the bottom, f ($=7.7\times10^{-4}$ s^{-1}) the Coriolis parameter, g ($=980$ cm s^{-2}) the acceleration of gravity, $\mathbf{k}$ the unit vector pointing positive upward, and ν_H ($=5.5\times10^5$ cm^2 s^{-1}) the constant horizontal eddy viscosity, respectively. τ is the bottom stress vector with components τ_x and τ_y in the x and y directions, respectively, and is assumed to be represented by a quadratic term with coefficient $\gamma_b{}^2$, i.e.,

$$\tau = (\tau_x,\tau_y) = -\gamma_b{}^2(u^2+v^2)^{1/2}\mathbf{u}, \quad (3)$$

where $\gamma_b{}^2$ is taken to be equal to 0.0026 after Hansen (1956). The barotropic water motion is derived from the tidal elevation of M_2 which is given along the open boundary by

$$\zeta = \zeta_b \sin[(2\pi/T)t], \quad (4)$$

where the amplitude ζ_b and period T of the M_2 tide are taken to be 90 cm and 12 lunar hours, respectively. The initial values of u, v and ζ are zero in the whole basin. The calculation is performed by using ADI method (Leendertse, 1971). The 1 km $\times$ 1 km finite-difference grid and a time step of 45 lunar seconds are used in the present tidal model. After integrating Eqs. (1) and (2) for five cycles of the M_2 tide, the model settles down to a stationary state.

Next we calculate the trajectories of marked particles moving in the above velocity field in a stationary state defined by the Eulerian coordinate system. It should be noticed that the position of a marked particle is determined by the Lagrangian system. If a marked particle moves from an initial position $\mathbf{x}_0$ at time t_0 to a new position $\mathbf{x} = \mathbf{x}_0 + \Delta\mathbf{x}$ at time t, then its Lagrangian velocity $\mathbf{u}_l\{\mathbf{x}(\mathbf{x}_0,t),t\}$ is given as:

$$\mathbf{u}_l\{\mathbf{x}(\mathbf{x}_0,t),t\} = \mathbf{u}(\mathbf{x},t) = \mathbf{u}(\mathbf{x}_0,t) + \Delta\mathbf{x}\cdot\nabla_H\mathbf{u}(\mathbf{x}_0,t). \quad (5)$$

Of course, Eq. (5) is correct only to order $\Delta\mathbf{x}$, and quantities of a higher order than $(\Delta\mathbf{x})^2$ are ignored. The new velocity of the marked particle depends on the space gradient $\nabla_H\mathbf{u}$ of the velocity field. Now, if $\Delta\mathbf{x}$ is very small compared to the local length scale of the velocity field, $\Delta\mathbf{x}$ can be given by

$$\Delta\mathbf{x} = \int_{t_0}^{t}\mathbf{u}(\mathbf{x}_0,t)\,dt$$

to the same approximation, and then the new position $\mathbf{x}(\mathbf{x}_0,t)$ is given by

$$\mathbf{x}(\mathbf{x}_0,t) = \mathbf{x}_0 + \int_{t_0}^{t} \left\{ \mathbf{u}(\mathbf{x}_0,t) + \int_{t_0}^{t'} \times \mathbf{u}(\mathbf{x}_0,t')dt' \cdot \nabla_H \mathbf{u}(\mathbf{x}_0,t) \right\} dt, \quad (6)$$

which is obtained from integrating Eq. (5) over a small time interval Δt $(=t - t_0)$. According to Longuet-Higgins (1969), if a marked particle is released in a periodic current and oscillates around the neighborhood of its initial position, the Lagrangian mean velocity of the marked particle is given by

$$\overline{\mathbf{u}_l\{\mathbf{x}(\mathbf{x}_0,t),t\}} = \overline{\mathbf{u}(\mathbf{x}_0,t)} + \overline{\int \mathbf{u}(\mathbf{x}_0,t)dt \cdot \nabla_H \mathbf{u}(\mathbf{x}_0,t)}, \quad (7)$$

where overbars denote the time average over the period of the periodic current, and the first term of the right-hand side represents the Eulerian mean velocity and the second term represents the Stokes velocity. Tee (1976) also discussed these velocities in the Minas Channel and the Minas Basin, using somewhat different formulations to those in Eq. (7) but their physical meanings are the same. Since the Lagrangian mean velocity in Eq. (7) indicates the mean flux past a fixed point, as a matter of course we must track the Lagrangian movement of a marked particle over a cycle by using Eq. (6). Moreover, the spatial change of the velocity of the tidal current is generally rapid in the vicinity of a strait (as is shown in Figs. 4 and 5) and, therefore, in order to increase the accuracy of the calculation of the Lagrangian movement, the trajectory of a marked particle must be successively calculated at every small time interval Δt.

In the present study we vary the magnitude of t (<3 min) as necessary, so that a particle does not move over the length of a grid box of 1 km during Δt. Marked particles are also labeled so as to be distinguished from one another and to evaluate the water volume exchanged through a strait. Nine particles per grid box are deployed initially; the arrangement is shown in Fig. 2. The velocity $\mathbf{u}(\mathbf{x}_0,t)$ in Eq. (5) is obtained from interpolating the Eulerian velocities of the tidal current calculated from a finite-difference grid. This technique is similar to that in the Marker and Cell method (Nicholas and Hirt, 1973) and is described in detail in the Appendix.

3. Preliminary analysis (mechanism of tidal exchange)

Prior to the representation of results obtained from the nonlinear system of the tidal current described in Eqs. (1) and (2), we will document some results of a preliminary analysis in order to facilitate the understanding of the mechanism of tidal exchange advocated in this paper.

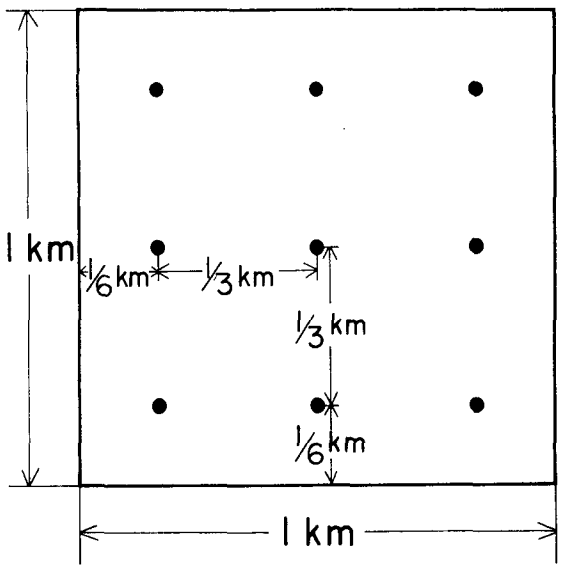

FIG. 2. The arrangement of labeled particles (●) in a grid box.

We assume a simple and artificial velocity field which is expressed as

$$u(y,t) = u_0(y) \cos\{[(2\pi/T)t] + \varphi(y)\}, \quad (8)$$

$$v(t) = v_0 \cos[(2\pi/T)t], \quad (9)$$

where $v_0 = 0.25$ m s^{-1} and T is the period of the M_2 tide. Fig. 3 shows the calculated trajectories of two particles A and B for the following four cases:

- $u_0 = 1.00$ m s^{-1}, $\varphi = \pi/4$: oscillation in the M_2 current without velocity shear and the spatial change of phase lag.
- $u_0 = 10^{-4}y$ m s^{-1}, $\varphi = \pi/4$: oscillation in a velocity field with only velocity shear.
- $u_0 = 1.00$ m s^{-1}, $\varphi = \pi/4 \times 10^{-4}y$ (y in m): oscillation in a velocity field with only the spatial change of phase lag.
- $u_0 = 10^{-4}y$ m s^{-1}, $\varphi = \pi/4 \times 10^{-4}y$ (y in m): oscillation in a velocity field with shear and the spatial change of phase lag.

In Fig. 3 black dots indicate the starting points of the particles in every tidal cycle, and solid and broken curves denote the trajectories during each former and each latter half cycle, respectively. The third and bottom panels clearly reveal that the spatial change of the phase lag has a similar effect on the movement of a particle to that of the velocity shear. We can clearly understand from these panels that the drift of a particle is induced by two important factors, i.e., velocity shear and the spatial change of phase lag. It should be noted that the movement of a particle calculated by Eq. (6) is nonlinear even if the velocity field is given by linearized forms of

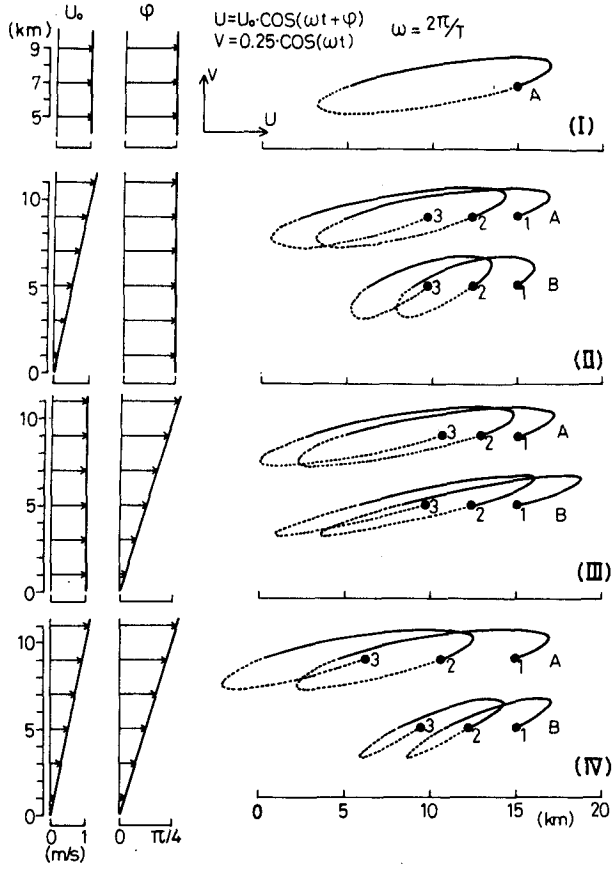

FIG. 3. The horizontal distributions of the amplitude and the phase lag of an artificial velocity field (the left side) and the trajectories of two marked particles (A and B) during two tidal cycles (the right side).

Eqs. (1) and (2), and therefore when only these factors exist, a particle does not return to its initial position after one tidal cycle.

Since in a coastal sea these two factors are determined by friction and the rapid variation of the coastal geometry, the drift of a water particle must be much larger in the vicinity of a strait than in the central area of a basin; as a result water exchange will take place between the inner and outer basins.

4. Results

The last tidal cycle in which the tidal model settles down to a stationary oscillation is used in the following analysis and discussion.

The amplitude and phase distributions of the u and v components of the calculated M_2 current are shown in Figs. 4 and 5, respectively. In the vicinity of the strait the amplitudes of both components are very large, sometimes over 2.5 m s^{-1}, and in addition their spatial changes are very rapid. The co-amplitude lines of relatively small amplitude extend from the strait to both basins asymmetrically. The spatial changes of the phase lag of both components are also rapid in the vicinity of the strait, especially the phase lag of the v component, which takes over 6 lunar hours between both ends of the strait. These are important points in regard to the velocity field of the M_2 current.

It is well known that the tidally-induced residual current is induced in the neighborhood of a strait by the nonlinear interaction of sinusoidal tidal current (Tee, 1976; Owen, 1980). It is defined as the velocity averaged over a cycle of the M_2 tide. Fig. 6 shows the distribution of velocity vectors of the tidally-induced Eulerian residual current obtained in this model. The apparent tidally-induced Eulerian residual circulations are found near the strait. The circulation in the outer basin is clockwise and that in the inner basin counterclockwise. The maximum velocity of the tidally-induced Eulerian current is 0.6 m s^{-1}.

We calculate the trajectories of a number of labeled particles in the above calculated velocity field. The calculation is started at the time of a maximum inward current at the center of the strait and is continued during a full cycle of the M_2 tide. Therefore, the labeled particles deployed in the strait at the initial time travel in both basins during one tidal cycle.

In order to clarify the roles of the M_2 and tidally-

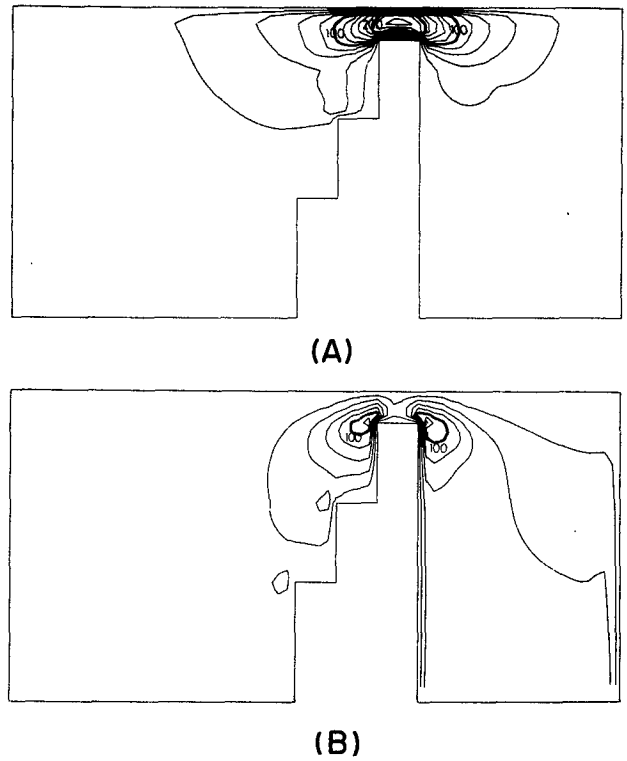

FIG. 4. The calculated M_2 co-amplitude lines (cm s^{-1}): (A) u component and (B) v component.

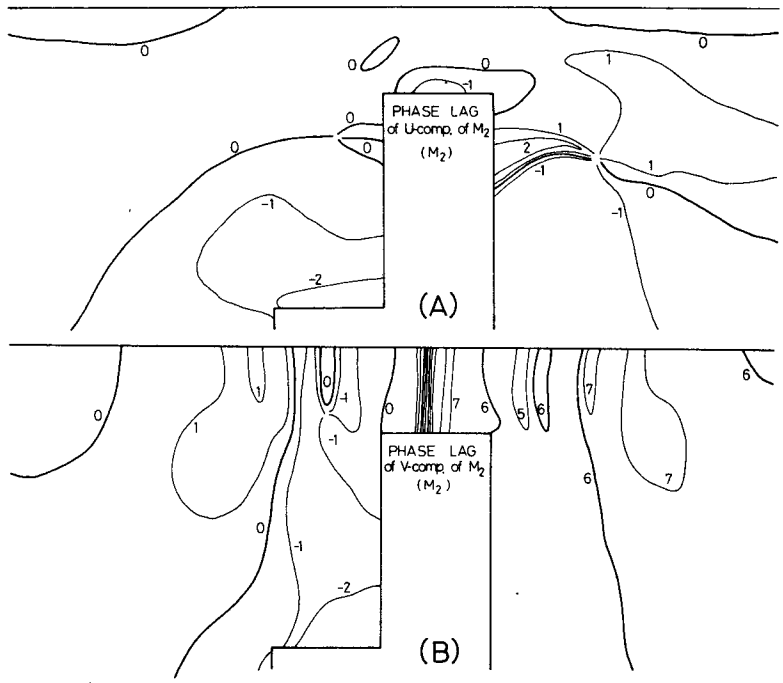

FIG. 5. The calculated M_2 co-phase lines (lunar hours): (A) u component and (B) v component.

induced residual currents in water exchange through the strait, we consider the following three cases of water exchange: (I) water exchange due only to the M_2 current, (II) water exchange due to both the M_2 and tidally-induced residual currents, and (III) water exchange due only to the tidally-induced residual current. Fig. 7 documents the states of the water exchanges in these three cases. Panel A shows the initial distribution of the inner (shaded part) and outer waters. Panels B and C show the transition of the water exchanges in cases I and II, respectively. The maximum volume of the outer water flowing into the inner basin occurs after 3 lunar hours; the maximum volume of the inner water flowing out of the inner basin occurs after 9 lunar hours. We can see that the exchange of considerably large amounts of water takes place in cases I and II. Panel D shows the water exchange after a cycle of the M_2 tide in case III. As the velocity of the tidally-induced residual current is small in the interior of the strait, as is shown in Fig. 6, then in case III the exchanged volume of water through the strait is very small, although it increases with time.

Next we consider why the large water exchange

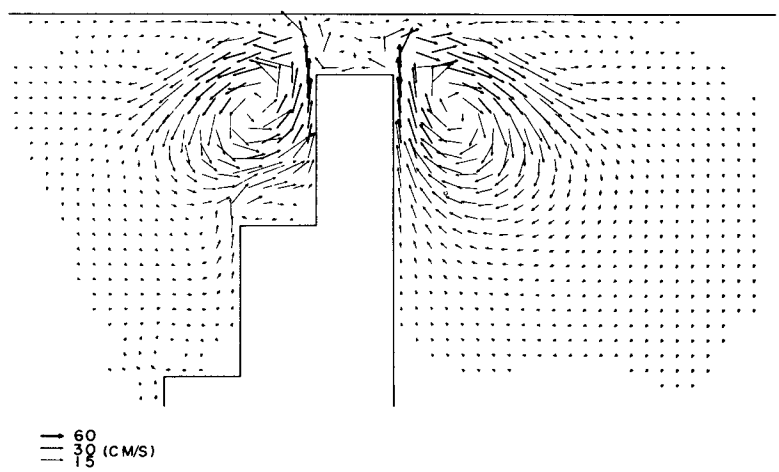

FIG. 6. The pattern of the tidally-induced Eulerian residual current.

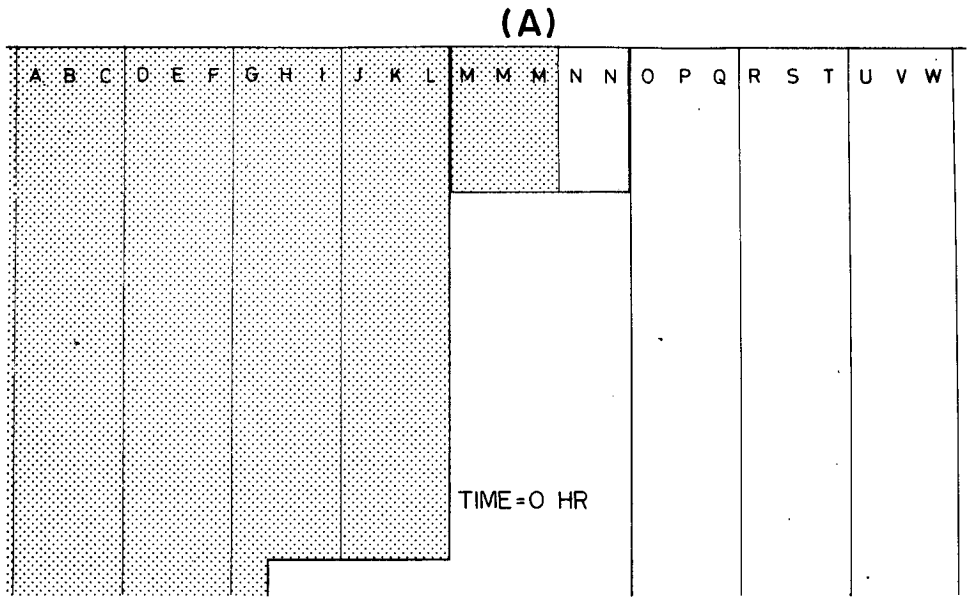

FIG. 7. (A) The initial state of the inner (shaded part) and outer waters, (B) and (C) the states of water exchange at every 1.5 lunar hours in cases I and II, respectively, and (D) the state of water exchange after a cycle of the M_2 tide in case III.

through the strait takes place in cases I and II. As has been observed in the preliminary analysis, the drifts of the particles in the vicinity of the strait become very large, because of the strong velocity shear and the rapid change in space of the phase lag of the M_2 current in that region (see Figs. 4 and 5). This situation can be clearly seen in Fig. 8, in which the trajectories of the representative particles in case II are shown; i.e., the drifts and tidal excursions of the particles initially released some distance from the strait are small, but those of the particles initially released in the vicinity of the strait are very large. Some of them pass through the strait and do not return to their home basins after one tidal cycle. As a result, fairly large amounts of water are exchanged between the adjacent two basins through the strait.

As is seen in Fig. 7 and Table 1, the water exchange in case II is the largest. This is obviously caused by the combination of three effects, i.e., the tidally-induced residual circulation, the large velocity shear, and the spatially rapid change of the phase lag of the M_2 current in the vicinity of the strait. The tidally-induced residual circulation plays the role of "shifter" in tidal exchange. It should be noticed that the sinusoidal M_2 current does not play only the role of "carrier" causing water particles to go and return between the inner and outer basins or carrying the particles to the tidally-induced residual circulations in both basins, as can be seen from the fairly large amount of water exchanged in case I. In other words, the Stokes drift of a particle moving in the M_2 current in the vicinity of the strait contributes more to the water exchange than the displacement of a particle due to the tidally-induced residual current.

5. Exchange ratio through a strait

As each labeled particle represents a water column, we can obtain the water volume exchanged between the inner and outer basins through a strait. Exchange ratio R indicating the magnitude of tidal exchange is defined as

$$R = V_{\text{res}}/V_{\text{max}}, \tag{10}$$

where V_{max} denotes the maximum volume of the outer water flowing into the inner basin through the strait over a cycle, and V_{res} the exchanged volume of the outer water into the inner basin after a cycle of the M_2 tide. It should be noted that V_{res} is not the net volume of water through a strait (see Fig. 9). In both cases I and II, V_{max} occurs after 3 lunar hours. The calculated values of the exchange ratio in cases I and II are listed in Table 1. In this study we do not discuss the exchange ratio in case III because of its negligible value compared with those in cases I and II, as can be deduced from Fig. 7D.

According to Table 1, the calculated exchange ratio in case I is ~40%, and that in case II ~87%. As the former value is about half the latter, we can see that the exchange of considerably large amounts of sea water takes place through the strait even in the case where the velocity field consists only of the M_2 current.

Compared with the previous values of an exchange ratio of 20–30% (Parker *et al.*, 1972; Kawamura *et al.*, 1975; and others), the present values may seem to be large. Probable reasons for the discrepancy between the present findings and the previous values of the exchange ratio are as follows. First of all the present definition of the exchange ratio is

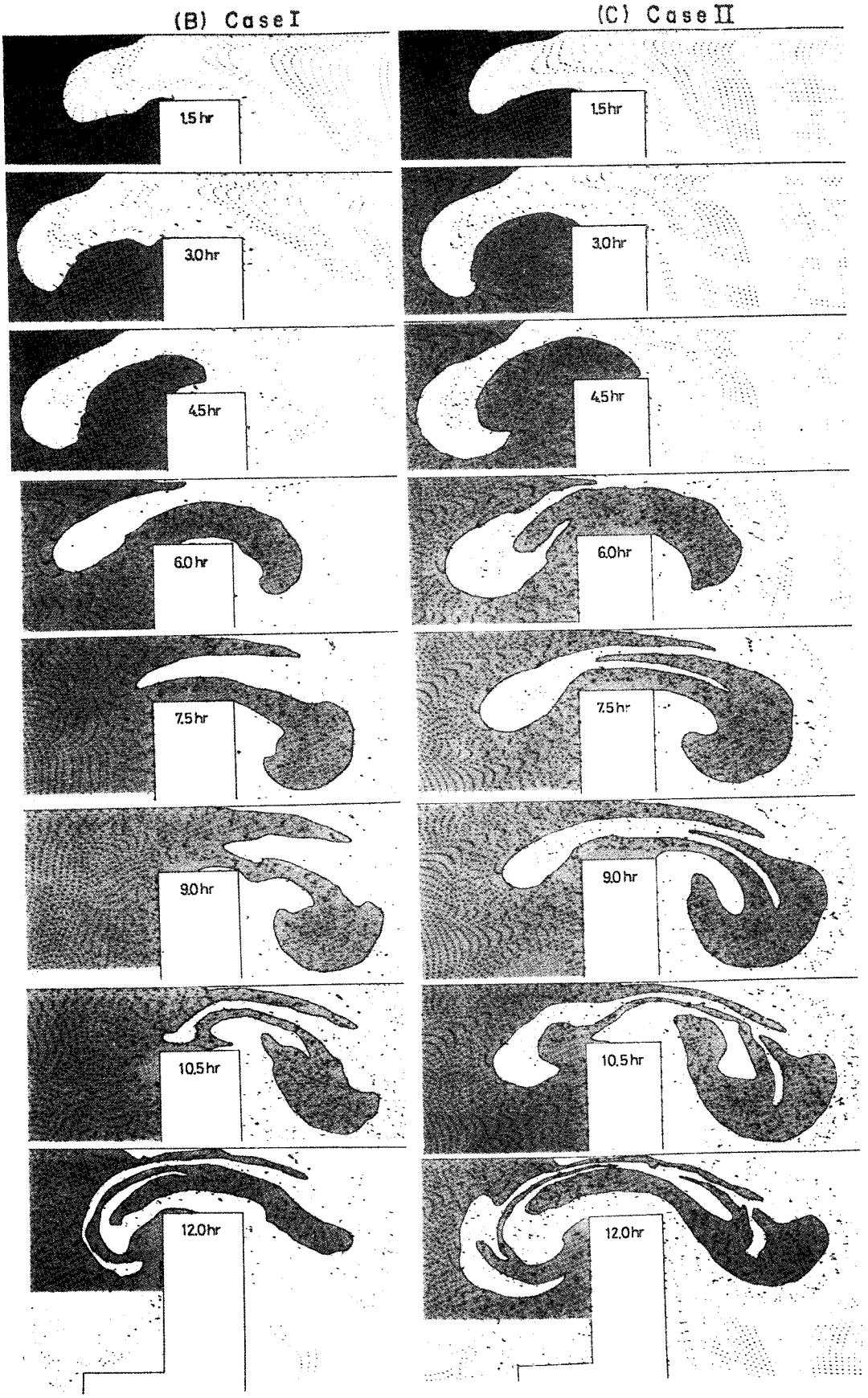

FIG. 7. (*Continued*)

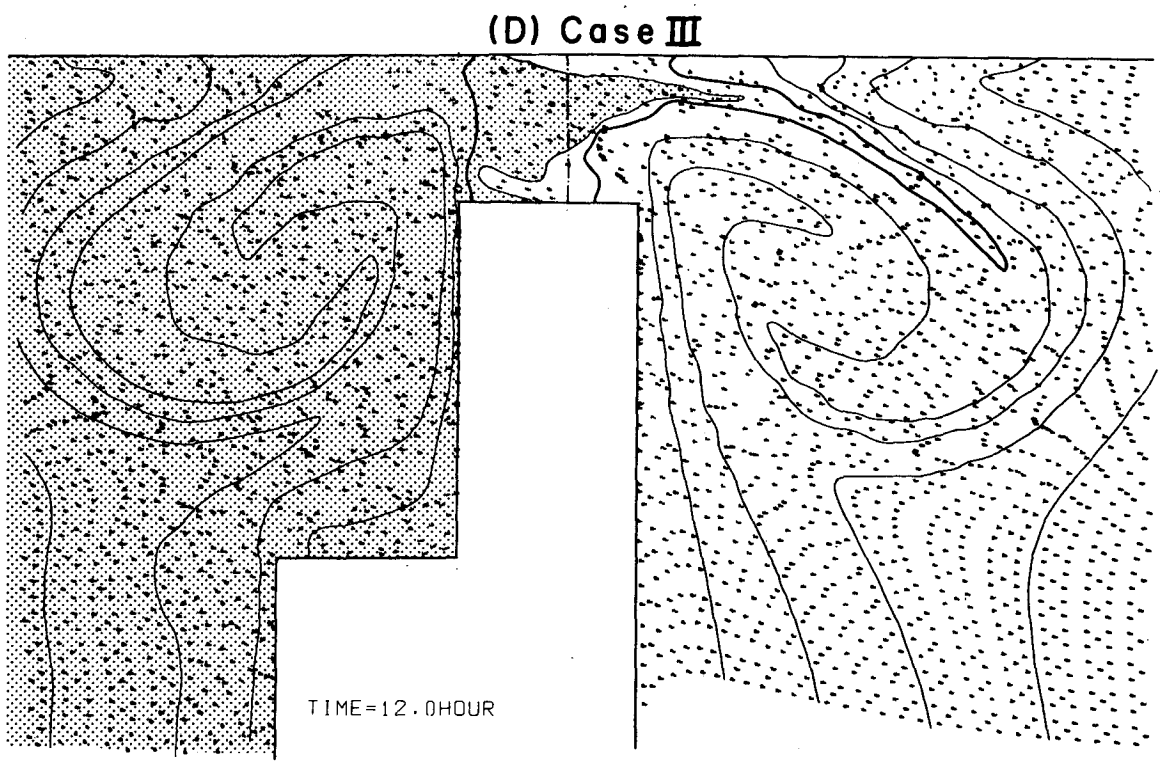

FIG. 7. (*Continued*)

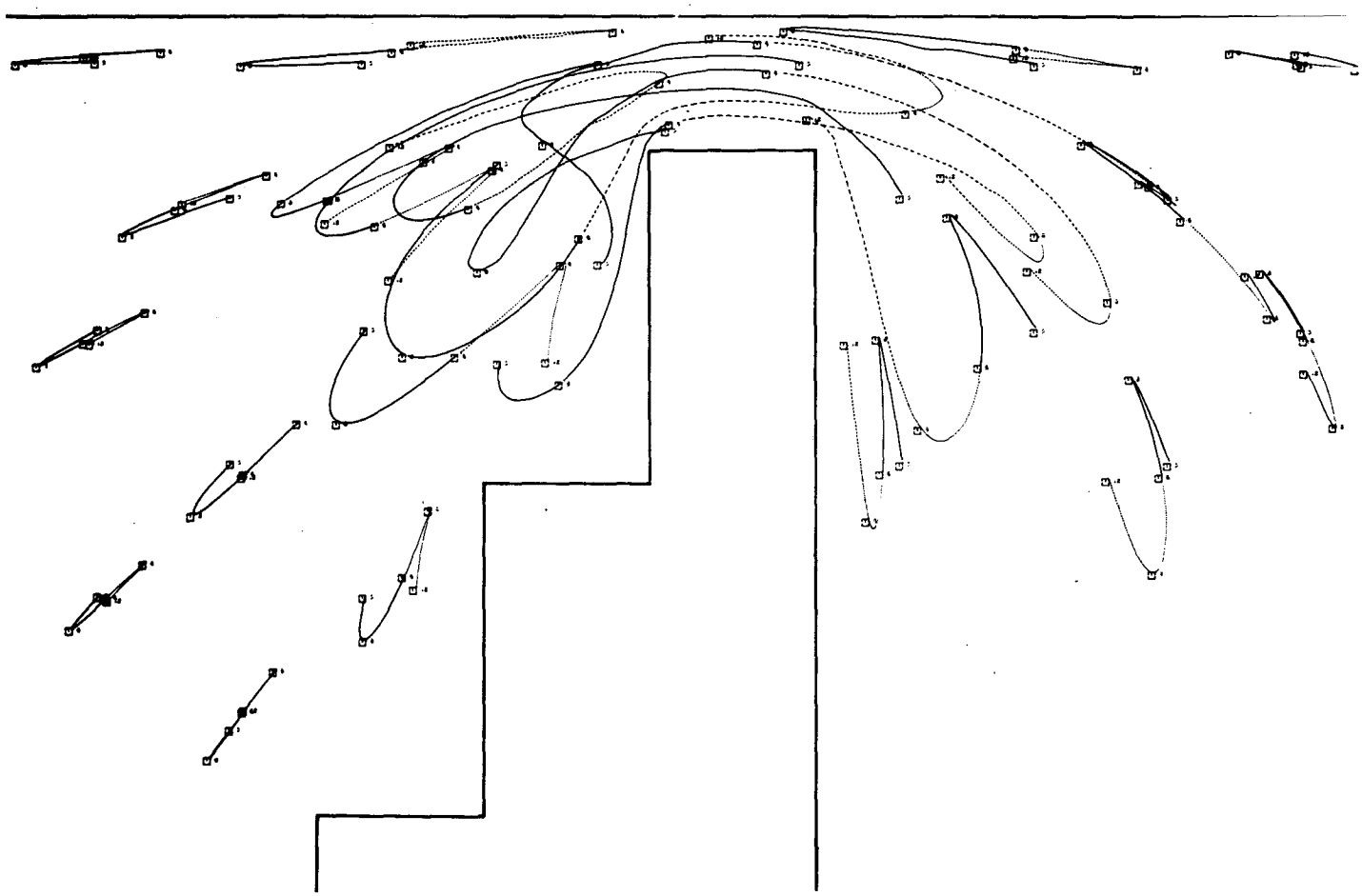

FIG. 8. The trajectories of several representative particles in the vicinity of the strait over a cycle. The solid and broken lines show the former and the latter half of the trajectories, respectively. The squares show the positions of the particles at every 3 lunar hours.

TABLE 1. The calculated values of the exchange ratio.

	Water volume (m^3)		Exchange ratio (%)
	V_{max} (3 h)	V_{res} (12 h)	
Tidal current	213×10^7	84.1×10^7	39.5
Tidal current + tidally-induced residual current	214×10^7	186×10^7	86.9

different from the previous ones. For example, Parker *et al.* consider the salinity distribution in a stationary state, and define the exchange ratio as that portion of the flood flow which is taken in with the flow for the first time (the outer water in the present definition). According to their definition, we would have to calculate the trajectories of the particles over many cycles of the M_2 tide. Kawamura *et al.* define the exchange ratio as that portion of the flood flow which is the bay water replaced by the outer water in a bay. Their definition contains an ambiguity, because in actual seas it is impossible not only to evaluate the salinities of the bay and outer water masses which are assumed to replace each other, but also to decide where those water masses come from. Finally, the exchange ratio depends on the structure of a velocity field, as has been clarified in this study, but we have no evidence regarding the effect of geometry or density stratification on tidal exchange in the actual basins studied by them.

In this paper we have obtained an extremely large value for the exchange ratio, but we must mention an important fact that V_{max}, in the present definition of the exchange ratio, is not concerned with the water volume which occupies the whole of the inner basin but with the volume of the outer water entering into the inner basin through a strait over a cycle.

We have discussed only the physical process of tidal exchange in a simple model basin with a simplified strait. As a matter of course, when we evaluate the flow and the distribution of water particles in a real coastal sea with a narrow strait, it will be necessary to use a relatively finer grid in the numerical tidal model in order to represent more adequately

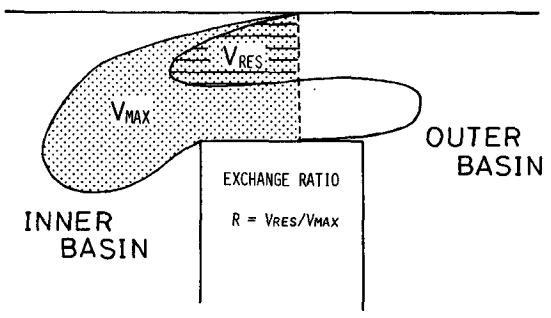

FIG. 9. Schematic view of V_{max} and V_{res}.

$\mathbf{u}\cdot\nabla_H\mathbf{u}$ in a strait and to calculate the Lagrangian movement of the particles, thereby allowing us to evaluate the water volume exchanged between two basins more accurately. An application of this method to an actual coastal sea will be published in the near future (Imasato *et al.*, 1980).

Acknowledgments. The numerical calculations in this paper were carried out on a FACOM M-190 in the Data Processing Center of Kyoto University.

APPENDIX

Calculation of Lagrangian Velocity

Assume a labeled particle at the position $\mathbf{X}(t_{m-1})$ at time $t = t_{m-1}$ (a solid circle in Fig. 10). Then the x-component velocity u, $\partial u/\partial x$ and $\partial u/\partial y$ at the position $\mathbf{X}(t_{m-1})$ are given by a weighted interpolation using the Eulerian velocity components of $U_{i,j}$, $U_{i+1,j}$, $U_{i,j+1}$ and $U_{i+1,j+1}$ (large solid arrows). The y-component velocity v, $\partial v/\partial x$ and $\partial v/\partial y$ at the position $\mathbf{X}(t_{m-1})$ are also given in the same way using $V_{i,j}$, $V_{i+1,j}$, $V_{i,j+1}$ and $V_{i+1,j+1}$ (large open arrows). The new position $\mathbf{X}(t_m)$ of the particle (a circle in Fig. 10) is calculated by Eq. (6). The successive position $\mathbf{X}(t_{m+1})$ of the particle in Fig. 10 is calculated by using the Eulerian velocities of $U_{i+1,j}$, $U_{i+1,j+1}$, $U_{i+2,j}$, $U_{i+2,j+1}$, $V_{i,j+1}$, $V_{i+1,j+1}$, $V_{i,j+2}$ and $V_{i+1,j+2}$. When the ith particle at the position $\mathbf{X}(t_{m-1})$ moves to a new position at a distance over the grid size of 1 km during the time interval $\Delta t = t_m - t_{m-1}$, the new position of the particle must be recalculated by integrating Eq. (6) from t_{m-1} to t_m with another small time interval such as $0.1 \times \Delta t$. Then no particle crosses the coastal boundary or jumps over the peninsula.

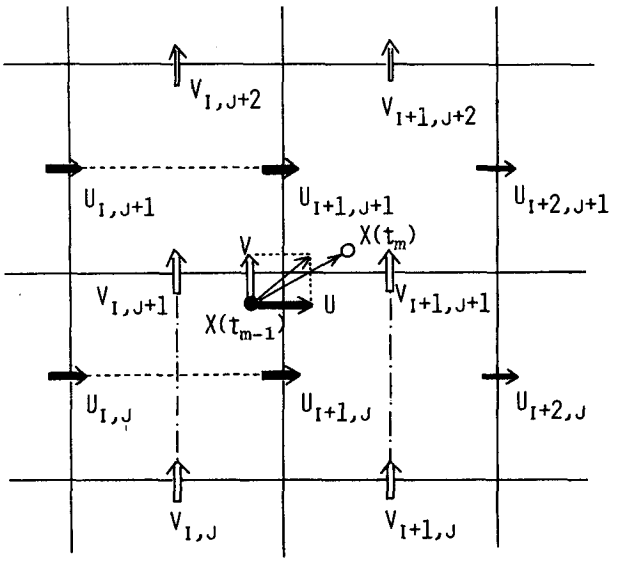

FIG. 10. Schematic diagram of the calculation of the particle motion.

REFERENCES

Hansen, W., 1956: Theorie zur Errechnung des Wasserstandes und der Strömungen in Rändmeeren nebst Anwendungen. *Tellus*, **8**, 287–300.

Imasato, N., T. Awaji and H. Kunishi, 1980: Tidal exchange through Naruto, Akashi and Kitan Straits. *J. Oceanogr. Soc. Japan*, **36**, 151–162.

Kawamura, M., K. Shimizu, H. Koyama, H. Nakajima and T. Maekawa, 1975: Hydrographic conditions and diffusion coefficient in the Bungo Channel. *Umi To Sola*, **50**, 43–58.

Leendertse, J. J., 1971: *A Water-Quality Simulation Model for Well-Mixed Estuaries and Coastal Sea*, Vol. 2. Rand Corp., 156 pp.

Longuet-Higgins, M. S., 1969: On the transport of mass by time-varying ocean currents. *Deep-Sea Res.*, **16**, 431–447.

Nakata, H., and T. Hirano, 1976: On the tidal transport and exchange of sea-water in Seto (strait) and approaches. *Bull. Japan Soc. Fish. Oceanogr.*, **29**, 7–14.

Nicholas, B. D., and C. W. Hirt, 1973: Calculating three-dimensional free surface flows in the vicinity of submerged and exposed structure. *J. Comput. Phys.*, **12**, 234–246.

Owen, A., 1980: The tidal regime of the Bristol Channel: A numerical modelling approach. *Geophys. J. Roy. Astron. Soc.* (in press).

Parker, D. S., D. P. Norris and A. W. Nelson, 1972: Tidal exchange at Golden Gate. *J. Sanitary Eng. Div., Proc. ASCE*, **98**, 305–323.

Tee, K. T., 1976: Tide-induced residual current, a 2-D nonlinear numerical tidal model. *J. Mar. Res.*, **34**, 603–628.